An Aerodynamic Optimization Framework for the Automotive Industry, based on Continuous Adjoint and OpenFOAM

E. Papoutsis-Kiachagias[1], V. Asouti[1], K. Giannakoglou[1], K. Gkagkas[2]

1) National Technical University of Athens, School of Mechanical Engineering, Parallel CFD & Optimization Unit, Iroon Polytexneiou 9, 157 73, Zografou, Athens
e-mails: vaggelisp@gmail.com, vasouti@mail.ntua.gr, kgianna@central.ntua.gr
2) Toyota Motor Europe NV/SA, Technical Center, Hoge Wei 33B, B- 1930 Zaventem, Belgium
e-mail: Konstantinos.Gkagkas@toyota-europe.com

I. Introduction

Aerodynamic optimization has been attracting the interest of both academia and industry and is gradually finding its way in day-to-day automotive industrial simulations. Among the various available optimization methods, gradient-based optimization coupled with the adjoint approach for computing the necessary sensitivity derivatives is extremely attractive for large scale optimization problems, due the ability of the latter to compute all the sensitivity components with a cost that is independent of their number. A framework for automated aerodynamic optimization has been developed by NTUA in OpenFOAM 2.3.1, using the continuous adjoint method as its building block. This framework allows for aerodynamic optimization of complex geometries using a single OpenFOAM executable called *adjointOptimization* and its accompanying libraries, performing all the required operations (flow and adjoint solution, geometry parameterization, grid displacement etc) in parallel and without relying on third-party tools. In the remainder of this abstract, the building blocks of the optimization framework are described and the code development undertaken is highlighted. After presenting the structure of the developed methods and software, an application targeting the multi-point, multi-objective optimization of a TOYOTA aerodynamics concept car is showcased.

II. Optimization Algorithm Components

The target of each optimization method is to minimize (maximize) a metric quantifying the performance of the analyzed aerodynamic shape; the latter is usually called the objective function of the optimization problem. A gradient-based optimization method requires a flow solver, a method to compute the sensitivity derivatives (SD), a technique to update the design variables based on the computed SD and, finally, a method to adapt or regenerate the computational grid after updating the geometry. The various components constituting *adjointOptimization* are briefly mentioned in this section. Where appropriate, the corresponding code developments of NTUA are highlighted.

a) Solution of the flow equations: The incompressible Navier-Stokes equations for steady or unsteady turbulent flows are solved, using the native OpenFOAM solvers (simpleFoam, pisoFoam etc). This, along with the solution of the corresponding adjoint equations, is the most computationally expensive part of the algorithm.

b) Computation of the objective function: After solving the flow (or primal) equations, the objective function(s) quantifying the performance of the geometry under consideration are computed. A wide variety of objective functions has been implemented, for external aerodynamics (forces, moments, approximation of turbulence induced aerodynamic noise), internal (ducted) flows (total pressure losses, power dissipation, mass flow rate partition) and turbomachines (hydraulic head, power, efficiency, target outlet velocity profiles, cavitation estimation [1]). The implemented objective function classes, apart from evaluating the objective value, also provide the environment for computing the contributions of the objective function differentiation to the adjoint boundary conditions and field adjoint equations. The code structure is such that the same OpenFOAM adjoint boundary condition types are applied by the user, irrespective of the objective function under consideration. The implemented adjoint boundary conditions, then, automatically receive the appropriate contribution by each objective function.

c) Solution of the adjoint equations: The adjoint equations to the incompressible RANS or URANS equations have been implemented in *adjointOptimization*. The developed code avoids the commonly made "frozen turbulence" assumption, based on which the variations of turbulence fields w.r.t. the design variables are neglected. Instead, the authors' group was the first to develop the (continuous) adjoint equations to low- and high-Re number turbulence models, including the Spalart-Allmaras [2], k-ω SST [3] and k-ε [4] turbulence models; the latter are included in *adjointOptimization* increasing the accuracy of the computed sensitivity derivatives [2]. An indispensable part of the adjoint system of equations when differentiating high-Re number turbulence models (i.e. those including wall functions) are the so-called adjoint wall functions, [2], used to compute the correct adjoint wall stresses. Differentiation of various source terms frequently met in industrial applications (porosity models, SRF and MRF source terms etc) are also included.

d) Computation of objective function sensitivity derivatives: After having computed the flow and adjoint fields, the computation of the sensitivity derivatives (SD) driving the optimization loop can be conducted. Even though up until recently this was considered a trivial step, recent research has shown that the way SD are computed, and especially whether grid sensitivities are accounted for or not, can have a profound effect on the SD accuracy [5]. Typical continuous adjoint approaches compute SD either through Surface Integrals only (the so-called SI approach) by neglecting grid sensitivities, with low cost but questionable accuracy, or through a combination of surface and Field Integrals (FI) including grid sensitivities, with high accuracy at a high CPU cost in the case of many design variables. In [5], the authors' group proposed a new SD approach, the so-called Enhanced Surface Integral (E-SI) one, which combines the low-cost of the

SI approach and the accuracy of the FI one. All three sensitivity formulations are included in *adjointOptimization*.

e) Update of the design variables: Once the sensitivity derivatives driving the optimization have been assessed, the update of the design variables can be computed. Some of most widely used algorithms, including conjugate gradient, SR1 and BFGS for unconstrained optimization and ALM, constrained projection and SQP for constrained optimization problems, [6], have been implemented within *adjointOptimization.* The continuous adjoint method is also used to compute the gradient of the constraint functions, when necessary.

f) Grid displacement and geometry parameterization: Once the update of the design variables has been computed, the aerodynamic shape can be updated and a new optimization cycle can begin. However, before doing so, the computational grid has to be adapted to the new, optimized geometry. Regenerating the grid is to be preferably avoided for reasons related to the high CPU cost of grid generation and interpolation inaccuracies taking place when transferring data from one grid to another. Hence, reliable methods able to adapt an existing grid to a new geometry should be available. Apart from using the grid adaptation methods already available within OpenFOAM, a number of methods have been developed and implemented within *adjointOptimization.* The most prominent ones are a grid displacement strategy based on the concept of linear elasticity [7] and a geometry parameterization and grid displacement tool based on volumetric B-Splines [8]. The latter, apart from adapting the grid after each optimization cycle, is also used as a free form deformation tool for the shape. Other forms of supported parameterization include NURBS curves (2D geometries) and surfaces (3D geometries).

III. Multi-Point, Multi-Objective Optimization of a TOYOTA Aerodynamics Concept Car

In this section, *adjontOptimization* is used to optimize a TOYOTA Aerodynamics Concept Car. The concept car represents a study of a visionary ultra-lightweight and efficient vehicle. As a result of the very low weight, wind gusts can have a more significant impact to the driving experience. It is therefore desirable to optimize the shape for reducing the sensitivity to side winds, while maintaining a very low drag coefficient. A polyhedral mesh consisting of approximately 1.6 Million cells (~7 Million points) is used. The steady-state Navier-Stokes equations coupled with the Spalart-Allmaras turbulence model with wall functions are solved in order to compute the flow field. In the final presentation, a comparison of the CFD-based aerodynamic coefficients with experimental values will be presented for a number of side-wind angles. The adjoint system includes the adjoint to the Spalart-Allmaras turbulence model as well as adjoint wall functions; sensitivity derivatives are computed using the FI approach. The goal of the optimization is to minimize the drag coefficient in axial flow and the yaw coefficient in the presence of a 30^o strong side-wind. Hence, a two-point, two-objective optimization problem is tackled. The flow chart of

the optimization algorithm is presented in Fig. 1. Two morphing boxes based on volumetric B-Splines are used to parameterize the spoiler and diffuser parts of the car, Fig. 2. The latter were identified as important for minimizing the drag and yaw coefficients, after computing the so-called sensitivity maps, Figs. 3 and 4. A symmetric displacement of the control points is enforced in the lateral direction, in order to maintain the car symmetry. Since gradient-based optimization methods must work with a single objective, the two targeted objectives are concatenated in one, using appropriate weights. Optimizing using different weight values leads to a collection of a number of points on the Pareto front of non-dominated solutions, Fig. 5. The different car shapes obtained for various weight values are depicted in Fig. 6. Two clear trends can be observed: a) increasing the spoiler height leads to a decreased yaw moment coefficient (at the same time increasing, however, the drag coefficient at the nominal condition) whereas increasing the diffuser length leads to a smaller drag coefficient.

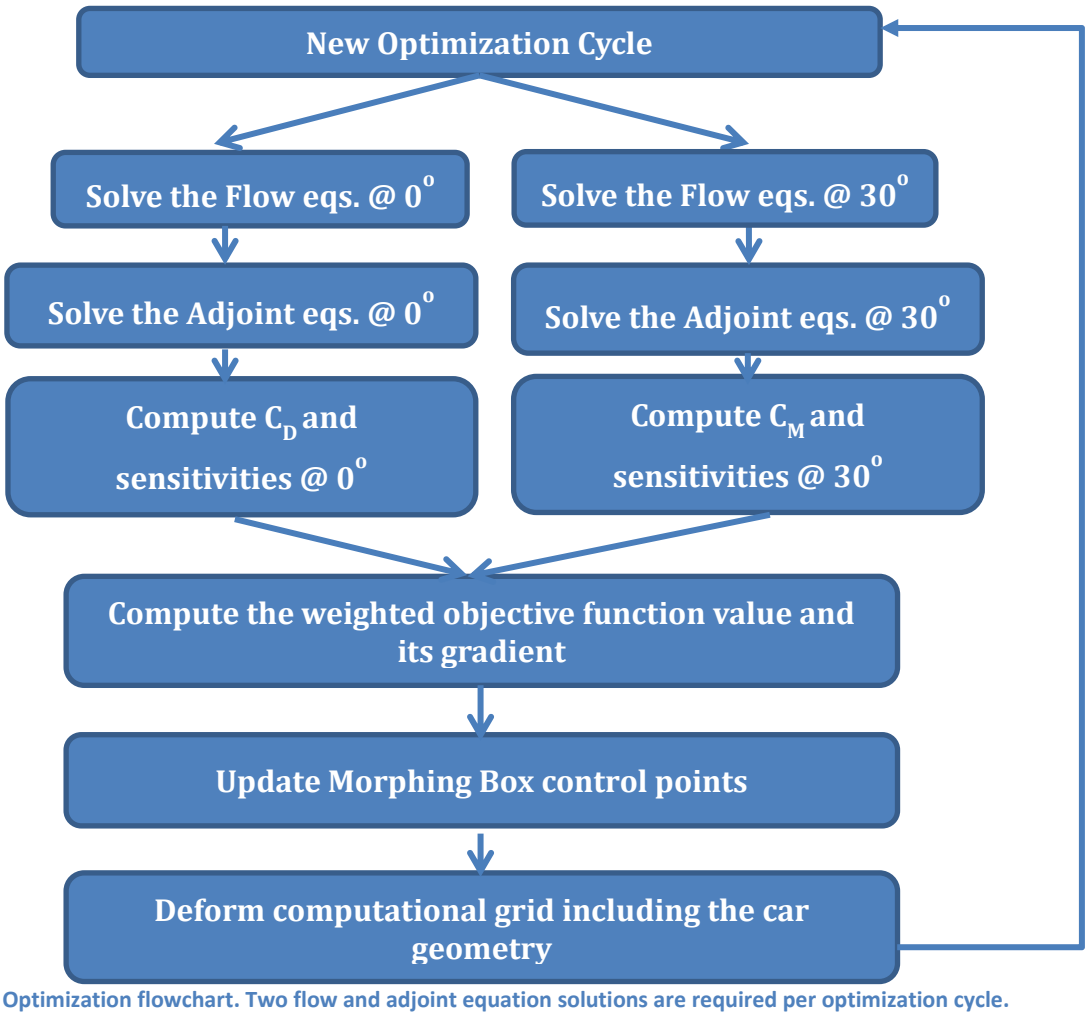

Figure 1: Optimization flowchart. Two flow and adjoint equation solutions are required per optimization cycle.

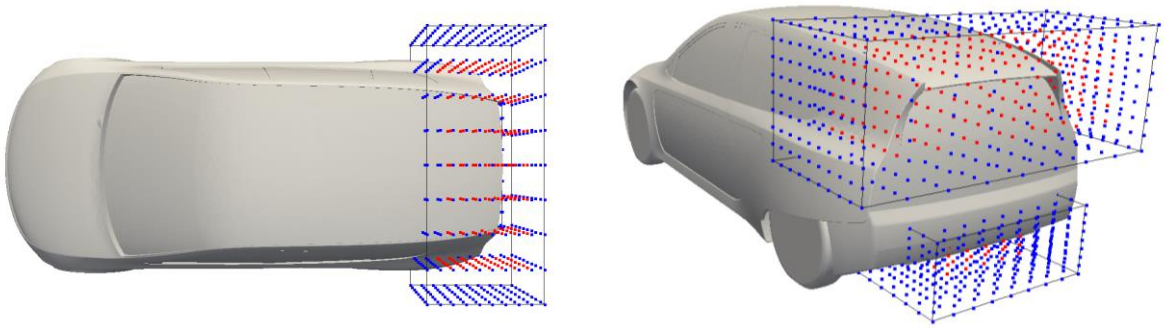

Figure 2: Morphing boxes used to parameterize the car surface. Control points colored in red are allowed to vary during the optimization while blue ones are kept fixed. Two morphing boxes with a total of 444 active control points are positioned in places where the sensitivity maps indicated a great optimization potential (see also Fig. 2).

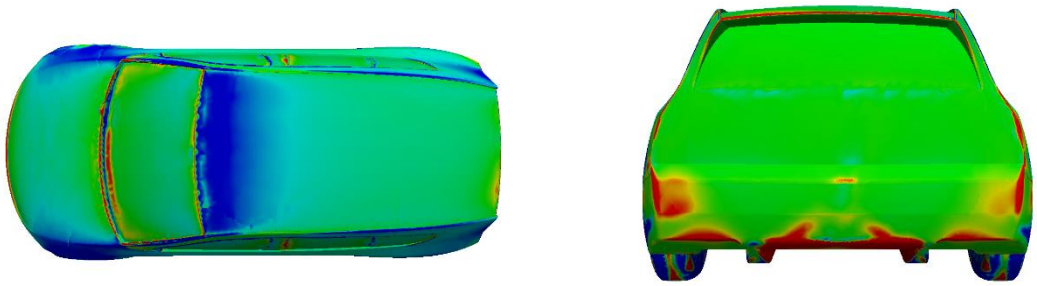

Figure 3: Drag sensitivity map computed for a 0^O flow, i.e. the sensitivity derivative of the drag coefficient w.r.t. the normal displacement of the boundary wall nodes. Red areas indicate an outward displacement in order to reduce drag whereas blue areas suggest the opposite. High (absolute)-valued sensitivity derivatives appear on the diffuser, making it a potential optimization candidate.

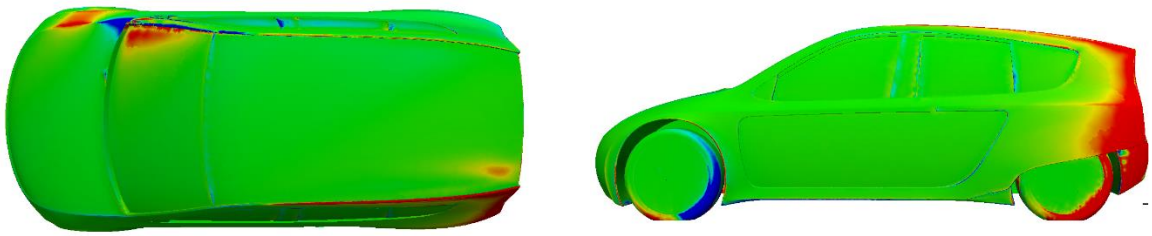

Figure 4: Sensitivity map of the yaw moment coefficient at 30^o side-wind. Color map as in Fig. 1. The spoiler and back side areas are identified as the ones with the highest optimization potential.

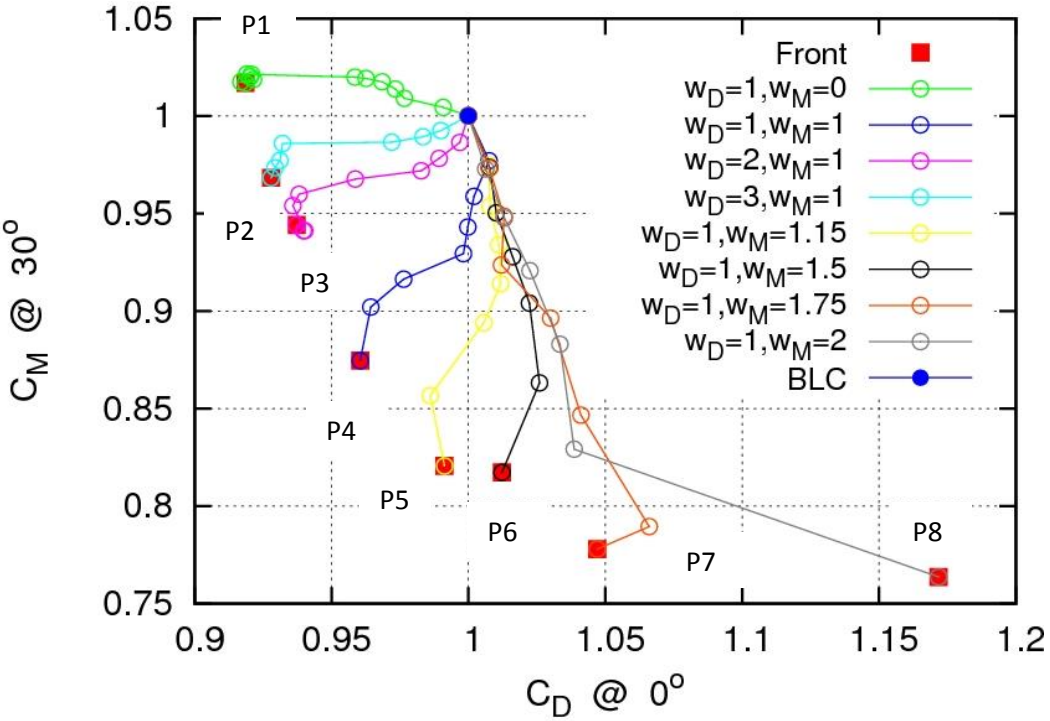

Figure 5: Convergence history of the optimization runs conducted using various weights for the drag (w_D) and yaw moment (w_M) coefficients. All values have been normalized with the values of the baseline car (BLC) geometry. The Pareto front on non-dominated solutions is marked in red. It is clear that at least four Pareto front members (P2 to P5) outperform the BLC geometry w.r.t. both objectives.

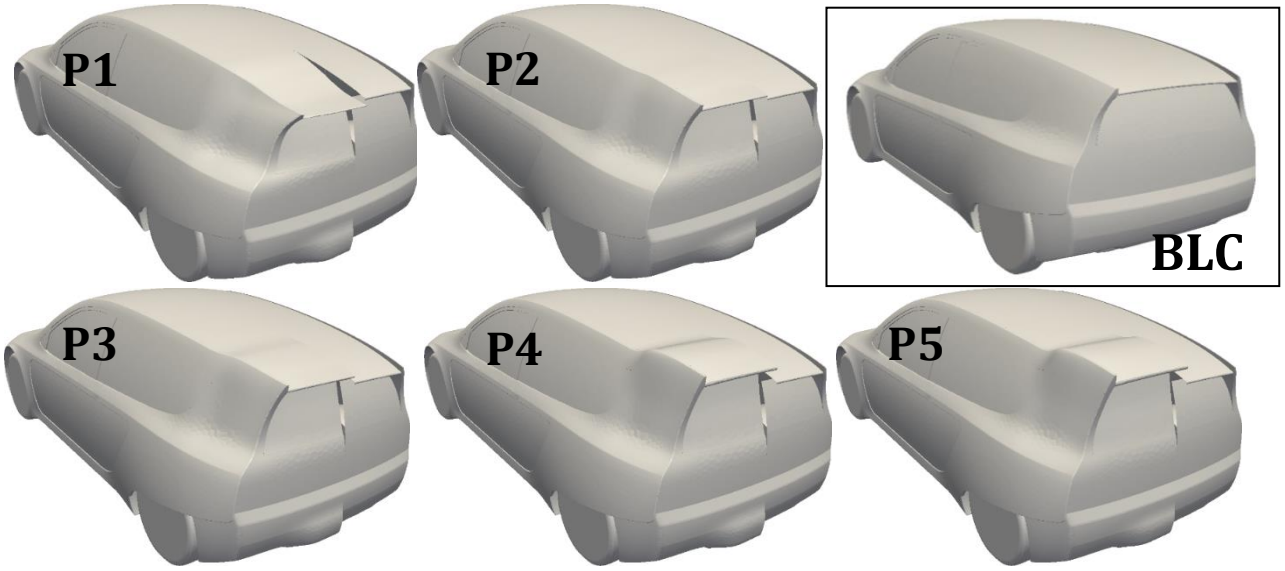

Figure 6: Some of the Pareto front members presented in Fig. 4. A higher spoiler height leads to reduced yaw moment @ 30°, increasing however drag @0°. Prolonging the diffuser helps to reduce drag @ 0°.

IV. Bibliography

1) E.M. PAPOUTSIS-KIACHAGIAS, S.A. KYRIACOU, K.C. GIANNAKOGLOU: The Continuous Adjoint Method for the Design of Hydraulic Turbomachines, Computer Methods in Applied Mechanics and Engineering, Vol. 278, pp. 621-639, 2014.
2) E.M. PAPOUTSIS-KIACHAGIAS, K.C. GIANNAKOGLOU: Continuous Adjoint Methods for Turbulent Flows, Applied to Shape and Topology Optimization: Industrial Applications, Archives of Computational Methods in Engineering, Vol. 23(2), pp. 255-299, 2016.
3) I.S. KAVVADIAS, E.M. PAPOUTSIS-KIACHAGIAS, G. DIMITRAKOPOULOS, K.C. GIANNAKOGLOU: The Continuous Adjoint Approach to the k-ω Turbulence Model with applications in shape optimization, Engineering Optimization, Vol. 47(11), pp. 1523-1542, 2015.
4) E.M. PAPOUTSIS-KIACHAGIAS, A.S. ZYMARIS, I.S. KAVVADIAS, D.I. PAPADIMITRIOU, K.C. GIANNAKOGLOU: The Continuous Adjoint Approach to the k-ε Turbulence Model for Shape Optimization and Optimal Active Control of Turbulent Flows, Engineering Optimization, Vol. 47(3), pp. 370-389, 2015.
5) I.S. KAVVADIAS, E.M. PAPOUTSIS-KIACHAGIAS, K.C. GIANNAKOGLOU: On the Proper Treatment of Grid Sensitivities in Continuous Adjoint Methods for Shape Optimization, Journal of Computational Physics, Vol. 301, pp. 1-18, 2015.
6) J. NOCEDAL, S. WRIGHT: Numerical Optimization, Springer, 1999.
7) R.P. DWIGHT: Robust Mesh Deformation using the Linear Elasticity Equations, Proceedings of the Fourth International Conference on Computational Fluid Dynamics, ICCFD4, Ghent, Belgium, 10–14 July 2006, pp 401-406, 2006.
8) M.J. MARTIN, E. ANDRES, C. LOZANO, E. VALERO: Volumetric B-Splines Shape Parametrization for Aerodynamic Shape Design, Aerospace Science and Technology, 37, pp. 26-36, 2014.